

MOCA: A Modular Object-Centric Approach for Interactive Instruction Following

<https://github.com/gistvision/moca>

Kunal Pratap Singh*
IIT Roorkee & GIST

ksingh@ee.iitr.ac.in

Suvaansh Bhambri*
IIT Roorkee & GIST

sbhambri@ee.iitr.ac.in

Byeonghwi Kim*
GIST

byeonghwikim@gm.gist.ac.kr

Roobeh Mottaghi
Allen Institute for AI
roobehm@allenai.org

Jonghyun Choi
GIST
jhc@gist.ac.kr

Abstract

Performing simple household tasks based on language directives is very natural to humans, yet it remains an open challenge for an AI agent. Recently, an ‘interactive instruction following’ task has been proposed to foster research in reasoning over long instruction sequences that requires object interactions in a simulated environment. It involves solving open problems in vision, language and navigation literature at each step. To address this multifaceted problem, we propose a modular architecture that decouples the task into visual perception and action policy, and name it as **MOCA**, a Modular Object-Centric Approach. We evaluate our method on the ALFRED benchmark and empirically validate that it outperforms prior arts by significant margins in all metrics with good generalization performance (high success rate in unseen environments). Our code is available at <https://github.com/gistvision/moca>.

1. Introduction

The prospect of having a robotic assistant that can carry out household tasks based on natural language instructions is a distant dream that has eluded the research community for decades. On recent progress in computer vision, natural language processing and visual navigation, several benchmarks have been developed to encourage research on different components of such assistants including navigation [2, 5, 4, 21], object interaction [45, 29], and interactive reasoning [8, 12] in simulated environments [20, 3, 28]. Recently, taking a step forward to model real world scenarios, ALFRED (Action Learning from Realistic Environments

* indicates equal contribution. This work is done while KPS and SB are on remote internship in GIST.

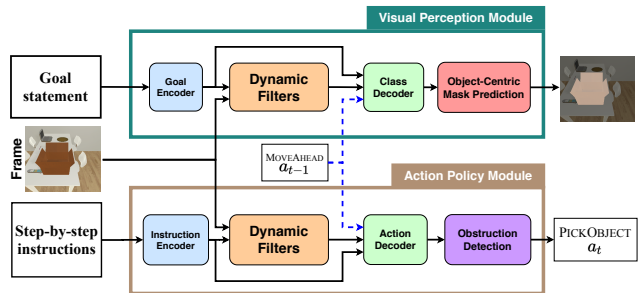


Figure 1: **Overview of MOCA.** It consists of the visual perception (VPM) and action policy modules (APM). The VPM predicts an interaction mask for the object that the agent interacts with using *object-centric mask prediction*. The APM predicts the current action of the agent. a_t and m_t denote the action and the interaction mask at time step t .

and Directives) [35] has been proposed to tackle an aggregated challenge of vision, language and navigation; following a long sequence of instructions while interacting with objects through egocentric visual observations to accomplish real-world household tasks such as *Put the pen from the cabinet drawer to the side table*. To alleviate the burden of such complex reasoning from a high level ‘goal statement’, ALFRED also provides low-level ‘step-by-step instructions’ that an agent must follow to achieve these goals. In addition, it also poses various realistic constraints such as long trajectory horizons, irreversible state changes, partial observability and egocentric vision which are individually open problems in the literature [45, 9, 5, 42]. Successful task completion requires addressing several individual challenges including pixel-level scene understanding and sequential action prediction with multi-modal information.

To address these multifaceted challenges in an end-to-end manner, we present a **Modular Object-Centric**

Approach, (MOCA) which is illustrated in Figure 1. Modularity addresses the bottlenecks in each aspect by well-defined individual components which are learned together in an end-to-end neural architecture. Specifically, we first decouple the two major yet distinct aspects involved in interactive instruction following, *i.e.*, policy and visual perception. The action policy module (APM) is responsible for sequential action prediction, whereas the visual perception module (VPM) generates pixel-wise interaction mask for the objects of interest for manipulation. As the VPM requires pixel-level understanding while APM abstracts the input to a single action label, we propose to learn them in separate branches (see Sec. 3.1).

The ability to interact with objects in the environment is central to interactive instruction following. Following [35], we let the agent to interact with objects by predicting a pixel-wise interaction mask of the target object. Accurate mask generation for an object of interest is crucial for successful task completion. Taking an object-centric viewpoint to it to ensure good localisation, we propose a class-aware mask prediction mechanism for interaction mask generation (Sec. 3.2). It bifurcates the task of interaction mask prediction into inferring the target object class and mask generation to ensure accurate pixel-level perception at every time step. We further improve the localizing ability in time by using the spatial relationship amongst the objects that are interacted with over consecutive time steps (Sec. 3.2.2).

Visual grounding by natural language is also an important building block in this task but unfortunately is one of the long-lived open problems in the literature [43, 33, 17, 16]. Inspired by the use of dynamic filters [18] to encode multi-modal information either with a single image or with a single sentence [11], we extend it to a continuous stream of varying visual observations and instructions (Sec. 3.3).

In addition, we observe that sometimes immovable objects like walls, tables, kitchen counters block the agent’s path and after multiple failed attempts to pass through them, the trajectory is declared as failed. To address this, we further propose an obstruction detection module in the APM. It detects when the agent is stuck around an obstacle and forces it to take an action to moves away from it (Sec. 3.4). Finally, we use a simple color swapping augmentation to curb the sample complexity of imitation learning, specifically behaviour cloning which is used to train our agent, MOCA. It is found to be particularly effective in training a good agent for our task (Sec. 4.2).

We empirically validate the proposed method, MOCA on the ALFRED benchmark [35] with all provided evaluation metrics. In comparison to prior arts that are either published or not, MOCA outperforms them by large margins on all metrics and ranks first in the public leaderboard¹ at the time

¹<https://bit.ly/2UrT3ur>, entry details: <https://bit.ly/3pyzHSK>

of submission.

2. Related Work

2.1. Embodied Grounded Language Learning

Vision and language navigation tasks require an agent to reach a goal by following natural or templated language instructions in a simulated environment through visual observations [2, 4, 5, 27]. [2] proposed the Vision-and-Language Navigation (VLN) task on the Room2Room (R2R) benchmark where an agent navigates on a fixed underlying navigation graph based on natural language instructions to reach the goal. Substantial improvements [41, 10, 26, 19, 25, 37, 23, 22] have been achieved on this benchmark by various proposals such as progress monitoring [25], augmenting trajectories via instruction generation [10] and environment dropout [37]. Recently, [21] proposed Vision and Language Navigation in Continuous Environments (VLN-CE) which lifts the assumption of known navigation-graph and perfect agent localisation from the R2R [2] benchmark. It also requires the agent to navigate via egocentric visual inputs as opposed to panoramic images. Both VLN and VLN-CE address the problem of navigation but ALFRED [35] requires an agent to navigate via egocentric visual observations and also interact with objects by producing a pixel-wise interaction mask to complete a task.

ALFRED [35] provides a high level *goal* statement and low-level step-by-step *instructions* that the agent needs to follow to accomplish a task. Shridhar *et al.* [35] proposed a Sequence-to-Sequence model with progress monitoring [25]. Even though such models perform reasonably well on VLN [2, 25], it does not generalize at all to unseen environments (near zero unseen success rate) indicating the difficulty of ALFRED as compared to previous benchmarks. Recently, Nguyen *et al.* [38] presented an approach where they relax the egocentric vision constraint of ALFRED by collecting multiple views per time step, essentially making it similar to panoramic views in VLN, then these visual features are processed via hierarchical attention with the step-by-step instructions. Recently, [36] presented TextWorld [7] based environments corresponding to embodied ones in ALFRED and named it as ALFWorld. Here, we propose to take a modular approach and show how decoupling various factors helps us analyze the bottlenecks involved and in turn helps us in learning an effective and superior performing agent on this benchmark. Note that we do not relax any constraints set of the original ALFRED benchmark and still outperform all existing methods [35, 38].

2.2. Visual Grounding

To accomplish the tasks on ALFRED [35], the agent needs to effectively interact with the right objects. Following [35], we perform object interaction by predicting

a pixel-wise interaction mask of the target object. This requires the agent to localise and produce a pixel-wise mask of the target object it intends to interact with. Visual grounding refers to localizing a specific object in an image using a natural language description. Previous methods leverage a pre-trained segmentation model [13, 46] to generate a set of candidate regions and either encode the visual and textual information separately using CNN-LSTM based methods [17, 15, 30, 44] or use a joint embedding [24, 33, 40, 6] to predict the best candidate proposal corresponding to the language query. [24, 33] reconstruct the language query based on joint vision and language features for better grounding. [43, 15] divide the input referring expression into modular phrases and process them using a modular attention network. Motivated by them we propose to split the interaction mask prediction into two stages; class prediction and mask generation (Sec. 3.2) and leverage a pre-trained instance segmentation model [13].

Previous works [6, 15, 30] have used simple arithmetic operations such as concatenation or element-wise product for grounding tasks but fail to fully capture the vision-language correspondence. [34, 31] have employed dynamic parameters for fully-connected layers and batchnorm statistics respectively for visual grounding. [39] use conditional batch-norm based on linguistic input for object tracking. [11] uses language query to predict hybrid convolution kernels for visual question answering. Contrary to these works, which operate in a static environment, we employ dynamic filters in an embodied environment with varied egocentric visual observations for the same language query over multiple time steps as further discussed in Sec. 3.3.

3. Approach

Towards building an instruction following AI agent in a near-realistic scenario, we use the ALFRED benchmark [35] to train and evaluate our model. It provides a high level *goal statement* (S_{goal}) and *step-by-step instructions* (S_{instr}) to accomplish each task. We tackle the problem of predicting low-level actions and pixel-wise interaction masks to achieve the goal in a modular fashion; separating them into individual branches but train the entire architecture in an end-to-end manner. For better visual-language grounding, we propose to employ language guided dynamic filters to help the agent generalise to unseen environments. Further, we propose a simple obstacle avoidance module that facilitates smooth navigation through the environment.

The objective function of our agent is as follows:

$$\mathcal{L} = - \underbrace{\sum_{t=1}^T y_t^c \log(p_{c,t})}_{VPM} - \lambda_a \underbrace{\sum_{t=1}^T y_t^a \log(p_{k,t})}_{APM} \quad (1)$$

$$+ \lambda_s \text{AL}_s(\mathbf{s}, \mathbf{s}^*) + \lambda_p \text{AL}_p(\mathbf{p}, \mathbf{p}^*),$$

where $p_{c,t}$ and $p_{k,t}$ denote the class probability and action probability, respectively. t and T denote the current time step and total trajectory duration respectively. y_t^a and y_t^c denote the GT action and class, respectively. VPM and APM denote visual perception module (Sec. 3.1.1) and action policy module (Sec. 3.1.2). Subgoal progress and overall progress sequences are denoted by \mathbf{s} and \mathbf{p} , respectively. \mathbf{s}^* and \mathbf{p}^* denote the GT subgoal and overall progress sequences. $\text{AL}_s(\mathbf{s}, \mathbf{s}^*)$ and $\text{AL}_p(\mathbf{p}, \mathbf{p}^*)$ are auxiliary subgoal and overall progress monitoring loss respectively same as [35]. λ_a , λ_s , and λ_p are the balancing hyper-parameters.

3.1. Decoupling Policy and Perception

Action prediction requires global semantic visual cues whereas visual perception for interaction requires local object specific features which enable precise localisation of the desired objects. On the language front, the low-level action-oriented information in step-by-step instructions is important for action prediction, whereas the object category information in the goal statement is sufficient for the mask prediction (*e.g.*, the interaction). The contrasting nature of the two tasks serves as a motivation for separating the branches for action and interaction mask prediction as shown in Figure 2. MOCA has two high level modules; the visual perception module (VPM) and action policy module (APM). Subscripts m and a indicate whether a component belongs to VPM or APM, respectively. We present a quantitative analysis of the benefits of this decoupling in Sec. 4.1 through input and model ablations.

3.1.1 Visual Perception Module (VPM)

The visual perception module (VPM) predicts the interaction mask of the object the agent wants to interact with. The VPM takes the visual features and the language features extracted by the goal encoder.

Action-conditioned visual perception. For capturing the cross-modal information between the goal statement and the visual observation at each time step, we use language guided dynamic filters for generating the attended visual features (Sec. 3.3 for details).

Additionally, we propose to use previous action embedding to predict the correct object along with the visual and language input. For example, in the goal statement, *Wash the spatula, put it in the first drawer*, the agent first needs to wash the spatula in the sink, for which we have two object classes, namely *spatula* and *sink* that the agent needs to interact with, but this has to be done in a particular order. Here the action information becomes important, *i.e.*, if the action is PUTOBJECT, the agent needs to predict the sink’s (receptacle) mask whereas if its PICKOBJECT, it needs to predict the spatula’s (object) mask. MOCA conditions the object interaction on the previous action embedding which helps

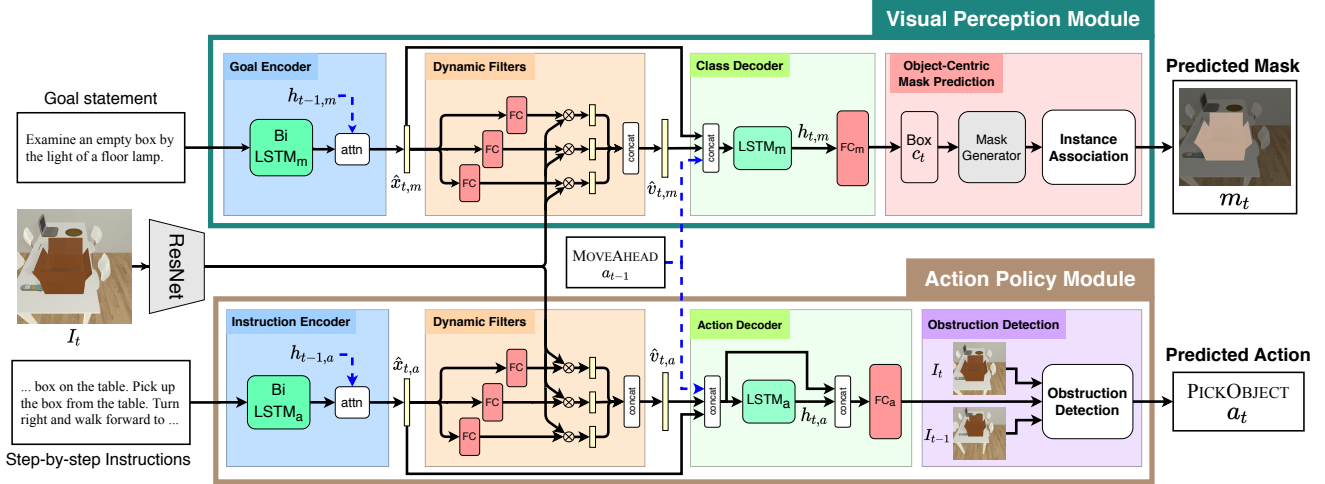


Figure 2: **Detailed architecture of MOCA.** The input frame, goal statement, and step-by-step instructions are denoted by I_t , S_{goal} , and S_{instr} , respectively. Subscripts m and a indicate whether a component belongs to VPM or APM, respectively. $h_{t,m}$ and $h_{t,a}$ denote hidden states of the class and action decoder, respectively. I_t is encoded by ResNet18. Dynamic filters convolve over the visual features, v_t , to give attended visual features, $\hat{v}_{t,goal}$ and $\hat{v}_{t,instr}$. The target class, c_t and action a_t are predicted on the basis of attended visual and language features with the previous action embedding. **Blue dashed lines** denote the input from the previous time step.

the agent to temporally align the object class with their corresponding interaction actions at the respective time step among multiple objects present in the goal statement. In summary, as shown in Figure 2, the hidden state $h_{t,m}$ of the class decoder, $LSTM_m$, is updated with three different information concatenated as:

$$h_{t,m} = LSTM_m([\hat{v}_{t,goal}; \hat{x}_{t,goal}; a_{t-1}]) \quad (2)$$

where $[\cdot]$ denotes concatenation. $\hat{x}_{t,goal}$ and $\hat{v}_{t,goal}$ are the attended language and visual features, respectively. The class decoder’s current hidden state $h_{t,m}$ is then used to predict the interaction mask m_t by invoking the *object-centric mask prediction* (Sec. 3.2).

3.1.2 Action Policy Module (APM)

We propose a module to predict the action sequence based on multi-modal information and call it as ‘action policy module’ (APM) depicted by the lower block in Figure 2. It takes visual features and step-by-step instructions but does not use the goal statement as input since it lacks low-level task-oriented information which is crucial for achieving the goal, unlike [35].

As illustrated in Figure 2, the attended language features are generated by the instruction encoder. Similar to VPM, we employ language guided dynamic filters for generating attended visual features (Sec. 3.3). Action decoder then takes attended visual and language features, along with the previous action embedding to predict the action decoder hidden state. After the action decoder hidden state is updated, a fully connected layer is used to predict the next

action, a_t as follows:

$$\begin{aligned} h_{t,a} &= LSTM_a([\hat{v}_{t,instr}; \hat{x}_{t,instr}; a_{t-1}]) \\ a_t &= \underset{k}{\operatorname{argmax}}(FC_a([\hat{v}_{t,instr}; \hat{x}_{t,instr}; a_{t-1}; h_{t,a}])), \quad (3) \\ k &\in [1, N_{action}], \end{aligned}$$

where $\hat{v}_{t,instr}$, $\hat{x}_{t,instr}$, a_{t-1} , and $h_{t,a}$ denote attended visual features, attended language features, previous action embedding and current action decoder hidden state, respectively. FC_a , takes as input $\hat{v}_{t,instr}$, $\hat{x}_{t,instr}$, a_{t-1} , and $h_{t,a}$ and predicts the next action, a_t . Note N_{action} denotes the number of actions. We keep the same action space as [35]. APM is further equipped by our obstruction detection (Sec. 3.4) mechanism. APM is trained using softmax cross entropy as shown in Equation 1.

3.2. Object-Centric Mask Prediction

In the VPM, we perform object interaction by predicting a pixel-wise interaction mask of the object of interest. Inspired by past work in language guided localisation [43, 17], we separate the task of interaction mask prediction into two stages; *target class prediction* and *instance association*. This bifurcation enables us to leverage the quality of pre-trained instance segmentation models while also ensuring accurate localisation. We refer to this mechanism as ‘object-centric mask prediction’, and it facilitates object manipulation for our agent. We ablate the effect of this component in Table 2 in Sec. 4.2.

3.2.1 Target Class Prediction

We take an object-centric viewpoint to interaction mask prediction by explicitly encoding the ability to reason about object categories in MOCA. To make the mask prediction object-centric, we first predict the target object class, c_t , that the agent intends to interact with at the current time step t .

Specifically, FC_m takes as input the hidden state, $h_{t,m}$, of the class decoder and outputs the target object class c_t , at time step t as shown in Equation 4. The predicted class is then used as an index for the mask generator to acquire the set of instance masks corresponding to the predicted class.

$$c_t = \underset{k}{\operatorname{argmax}} FC_m(h_{t,m}), \quad k \in [1, N_{class}], \quad (4)$$

where $FC_m(\cdot)$ is a fully connected layer and N_{class} denotes the number of the classes of a target object. The target object prediction network is trained as a part of the VPM with softmax cross-entropy loss with ground-truth object class as supervision. Note that VPM and APM are trained together in an end-to-end manner to align the predicted objects with their corresponding interaction actions.

3.2.2 Instance Association in Time

During inference, we employ a two-way criterion to select the best instance mask; ‘confidence based’ and ‘association based.’ If the agent interacts with an object for the first time, *i.e.*, the target object class between successive time steps is different, we pick the instance mask with the highest confidence score of mask prediction (‘confidence-based’). We use a pre-trained mask generator to obtain the instance masks and confidence scores, $\{(m_{i,c_t}, s_{i,c_t})\}_{i=1}^{M_t}$, where i and M_t denote the index and the number of predicted instance masks respectively for the target object class c_t predicted by our agent at the current time step. This ensures that the best possible mask from our mask generator is predicted and our agent does not interact with wrong objects.

On the other side, if the agent intends to interact with the same object instance over an interval, *i.e.*, the same object class is predicted over consecutive time steps (‘association-based’). For instance, as illustrated in Figure 3, an agent is trying to open a drawer and put a knife in it, the drawer selected for putting the knife must be the same one which was opened in the previous time step. To ensure this, we select the instance mask with the shortest Euclidean distance between its center and the center of the instance mask selected in the previous time step. The ‘association based’ selection criterion ensures to pick the same instance to interact with over consecutive time steps, even though its confidence may not be the highest over that period. In summary, instance association predicts the current time step’s interaction mask $m_t = m_{\hat{i},c_t}$ with the center coordinate, $d_t^* = d_{\hat{i},c_t}^*$, where \hat{i}

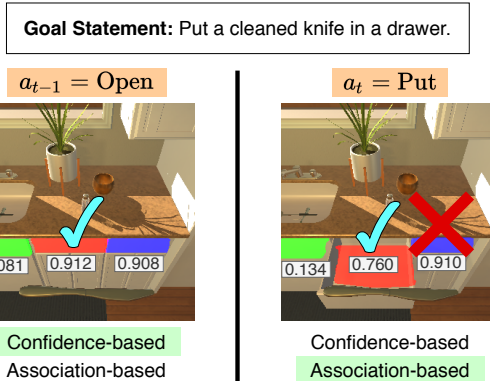


Figure 3: **Qualitative illustration of ‘Instance Association in Time’.** The generated masks of the drawers are labelled red, green, and blue with their corresponding confidence scores. ✓ denotes the target object interacted with at that time step. ✗ denotes that the target object with the highest confidence score is replaced by Instance-Association in Time. Using single-fold confidence-based approach makes the agent interact with different drawers over consecutive time steps as the closed drawer has higher confidence score. Instance-Association in Time helps the agent to interact with the same drawer over time and place the knife in it.

is obtained as:

$$\hat{i} = \begin{cases} \underset{i}{\operatorname{argmax}} s_{i,c_t}, & \text{if } c_t \neq c_{t-1}, \\ \underset{i}{\operatorname{argmin}} \|d_{i,c_t} - d_{t-1}^*\|_2, & \text{if } c_t = c_{t-1}, \end{cases} \quad (5)$$

where c_t is the predicted target object class and d_{i,c_t} the center coordinate of a mask instance, m_{i,c_t} , of the predicted class. Table 3 in Sec. 4.2 ablates instance association in time to highlight its empirical significance.

3.3. Language Guided Dynamic Filters

It is a straightforward and a common practice to concatenate the flattened visual and language features when addressing the two modalities of vision and language [17, 35, 15]. However, this naïve approach often fails to capture vision-language correspondence, which bottlenecks the performance in unseen environments [35].

To improve the generalization of our agent, MOCA, to *unseen* environments, we propose to use language guided dynamic filters to capture the spatial information attended on the language instructions. Dynamic filters [18] have been successfully applied in various downstream vision-language modelling tasks such as VQA [11] and natural language moment retrieval methods [32].

Contrary to these tasks which are performed either with a single image or a single sentence for a predetermined video sequence, our task has varying visual observations and language features at each time step. Thus, we extend the usage of the dynamic filters to generate kernels which attempt to capture various aspects of the language from the attended

language features. These Dynamic kernels are convolved with the visual features to obtain attended cross-modal feature maps as shown in the ‘Dynamic Filters’ block of Figure 2. The filter generator network, f_{DF} , takes the language features, x , as input and produces N_{DF} dynamic filters. These filters convolve with the visual features, v_t , to output multiple joint embeddings, $\hat{v}_t = DF(v_t, x)$ as follows:

$$\begin{aligned} w_i &= f_{DF_i}(x), \quad \forall i \in \{1, \dots, N_{DF}\}, \\ \hat{v}_{i,t} &= v_t * w_i, \\ \hat{v}_t &= [\hat{v}_{1,t}; \dots; \hat{v}_{N_{DF},t}], \end{aligned} \quad (6)$$

where N_{DF} , $*$ and $[\cdot]$ denote the number of dynamic filters, convolution and concatenation operation, respectively.

This multimodal encoding helps the agent to better utilise the correspondence between underspecified natural language instructions and visual features in unseen environments, thereby reducing the agent’s dependence on a particular modality. The dynamic filters are conditioned on the language features which makes them more adaptive and flexible towards varying inputs while performing tasks in unseen environments. This is in contrast with traditional convolutions which have fixed weights after training and hence cannot adapt according to the input. We empirically investigate the benefit of using language-guided dynamic filters in Sec. 4.2.

3.4. Obstruction Detection

It is observed that our agent, MOCA, tends to get stranded around immovable obstacles which eventually leads to trajectory failure. To mitigate this, we propose an obstruction detection mechanism in the APM to avoid obstacles. While navigating to a certain location, at every time step, the agent computes the difference between the observation at the current time step, I_t , and the previous time step, I_{t-1} with a tolerance hyper-parameter ϵ as following:

$$\|I_1 - I_2\|_1 < \epsilon. \quad (7)$$

When this equation holds and agent predicts the same navigation action over consequent time steps and fails to move through an object, the agent detects it as an obstruction. When an obstruction is detected, the agent’s action space is narrowed down to two navigation actions, *i.e.*, $\{\text{ROTATELEFT}, \text{ROTATERIGHT}\}$ to let the agent escape from the obstacle as illustrated in Figure 4. We empirically investigate its effect in Sec. 4.2.

4. Experiments

Dataset For near-realistic simulation of the interactive instruction following task, we use ALFRED benchmark that is running in the AI2-THOR [20] virtual environment. The

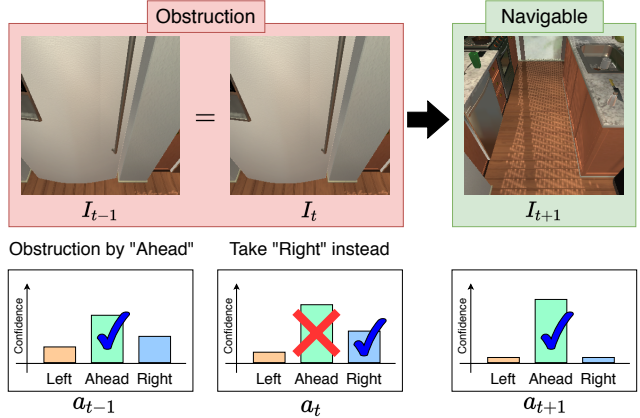


Figure 4: **Obstruction detection.** ✓ denotes the action taken at that time step. The MoveAhead action marked by × shows that our agent detects an obstruction at time step t by comparing previous and current observations, I_{t-1} and I_t . Therefore, instead of taking the MOVEAHEAD action again, our agent predicts the ROTATERIGHT action to detour it.

scenes in AI2-THOR are partitioned into ‘train’, ‘validation’ and ‘test’ sets. To evaluate the generalization ability of an agent, the validation and test scenes are split into two sections; *seen* and *unseen* folds.

Evaluation metrics. We follow the evaluation metrics proposed in [35], *i.e.*, Success Rate, denoted by *Task* and Goal Condition Success rate, denoted by *Goal-Cond*. Additionally, to measure the efficiency of an agent, the above metrics are penalized by the length of the sequence to compute a path-length-weighted (PLW) score for each metric [1]. For more details on evaluation metrics refer to [35].

Implementation details. The egocentric visual observations are resized to 224×224 . For the visual encoder, we use a pre-trained ResNet-18 [14]. For the mask generator, we use a Mask R-CNN [13] which takes a 300×300 visual observation and outputs the instance masks with 119 object classes along with confidence scores.

For training the Mask-RCNN, we use 2.1M frames and corresponding instance segmentation masks collected from replaying the training set expert trajectories are used. Note that we do not use any frame or segmentation masks from validation or test trajectories for Mask R-CNN training. MOCA is trained end-to-end using Adam with an initial learning rate of 10^{-4} and a batch size of 4 for 50 epochs. Balancing hyper-parameters in (1) are set as $\lambda_a = 1.0$, $\lambda_s = 0.2$, and $\lambda_p = 0.2$. We will release our code and pre-trained agents publicly.

4.1. Quantitative Analysis

We first conduct quantitative analysis of the performance on task success rate (Task) and goal-condition success rate

Model	Validation				Test			
	Seen		Unseen		Seen		Unseen	
	Task	Goal-Cond	Task	Goal-Cond	Task	Goal-Cond	Task	Goal-Cond
Shridhar <i>et al.</i> [35]	3.70 (2.10)	10.00 (7.00)	0.00 (0.00)	6.90 (5.10)	3.98 (2.02)	9.42 (6.27)	0.39 (0.80)	7.03 (4.26)
Nguyen <i>et al.</i> [38]	N/A	N/A	N/A	N/A	12.39 (8.20)	20.68 (18.79)	4.45 (2.24)	12.34 (9.44)
MOCA (Ours)	19.15 (13.60)	28.50 (22.30)	3.78 (2.00)	13.40 (8.30)	22.05 (15.10)	28.29 (22.05)	5.30 (2.72)	14.28 (9.99)
Input Ablations								
No Language	2.68 (1.30)	9.58 (6.30)	0.00 (0.00)	6.65 (3.00)	1.04 (0.77)	7.00 (4.70)	0.26 (0.05)	6.68 (3.63)
No Vision	0.24 (0.10)	5.88 (4.70)	0.00 (0.00)	7.17 (6.10)	0.00 (0.00)	4.36 (3.28)	0.39 (0.13)	7.46 (4.37)
Goal-Only	5.37 (2.70)	14.32 (10.00)	0.24 (0.10)	8.49 (4.80)	3.65 (1.99)	10.55 (7.68)	1.37 (0.47)	9.03 (5.40)
Instructions-Only	4.15 (2.60)	12.75 (9.60)	0.49 (0.30)	7.45 (5.30)	5.81 (3.60)	11.49 (8.99)	0.59 (0.25)	7.44 (4.46)
Human	-	-	-	-	-	-	91.00 (85.80)	94.50 (87.60)

Table 1: **Task and Goal-Condition Success Rate.** For each metric, the corresponding path weighted metrics are given in (parentheses). The highest values per fold and metric are shown in blue. ‘N/A’ denotes ‘not available’ as the scores are not reported in the leaderboard.

(Goal-Cond) and summarise the results in Table 1 with previous methods. As shown in the figure, MOCA shows significant improvement over the previous methods [35, 38] on all metrics. The higher success rate in the unseen scenes indicates its ability to generalize in novel environments. We achieve a relative improvement of 77.96% in Seen Task SR and 19.10% in Unseen Task SR over Nguyen *et al.* [38] that won ALFRED challenge in ECCV 2020.

MOCA outperforms them in both *Seen* and *Unseen* ‘Goal-Condition’ metrics and gives a relative improvement of 36.79% and 15.72%, respectively. It implies that our method improves the agent’s general understanding for all sub-tasks required for the successful completion of a task. As indicated in the parenthesis in Table 1, our approach provides better Path Length Weighted results for all the metrics which shows the efficiency of the agent’s performance. We also present sub-goal ablation in the supplementary.

4.2. Ablation Study

Input ablations. We ablate the inputs to our model in Table 1 to investigate the vision and language bias of our agent. When the agent is only given visual inputs (*No Language*) without goal and step-by-step instructions, we observe that the agent is still able to perform some tasks in the seen environments by memorising familiar visual and target class sequences, but fails to generalize on the unseen fold.

No Vision setting is able to achieve some goal condition success by following navigation instructions, but the lack of the visual input handicaps the interaction ability of the agent, thereby preventing it to achieve any success on both seen and unseen environments.

The *Goal-Only* setting highlights the ability of our agent to utilise the goal-statement better as compared to Shridhar *et al.* [35]. Since the Action Policy Module (APM) of MOCA does not utilise the goal-statement because of its lack of low-level action-specific information, the action prediction ability of this setting is equivalent to the *No-Language* setting. However, since the goal-statement

is used in the Visual Perception Module (VPM), it allows the agent to perform accurate object interaction and hence achieves much better performance than *No-Language*. This result is a direct benefit of the policy and perception decoupling discussed in Sec. 3.1.

Instruction-Only ablation in Table 1 indicates the performance when the agent does not receive the goal-statement. The low-level instructions drastically improve the action prediction ability over the *Goal-Only* setting as the APM can now leverage the low-level action information. However, the VPM is deprived of its language input which depletes the target-class prediction ability (Sec. 3.2.1) of the object-centric mask prediction module. This results in numerous failed interactions and thus it performs worse than MOCA and *Goal-Only* setting.

It is interesting to note that despite using either one of step-by-step instructions (*Goal-Only*) or goal statement (*Instructions-Only*), MOCA is still able to outperform [35] on all the metrics as shown in Table 1. This highlights the flexibility and robustness of our modular architecture which helps the agent to fully exploit each language input which is pivotal for achieving good performance on ALFRED. We would also like to highlight that for input ablations, the agent is deprived of the dynamic filters for either APM or VPM, or both, due to which the agent fails to perform well on unseen environments in all the input ablation settings.

Model ablations. To investigate the significance of each module with empirical studies, we perform a series of ablation studies on MOCA and summarize the results in Table 2. We begin by removing color swap augmentation which reduces the performance on all metrics which highlights its importance in training a better agent by curbing the sample complexity of imitation learning. We use the non color-swap variant to ablate over various modules for further analysis due to computational constraints.

Second, we remove the language guided dynamic filters (Sec. 3.3). The ablated model leads to a significant decrease in both seen and unseen metrics. This drop can be attributed

Components				Validation-Seen		Validation-Unseen	
Decoupling Policy & Perception	Object-centric Mask Prediction	Dynamic Filters	Color Swap	Task	Goal-Cond.	Task	Goal-Cond.
✓	✓	✓	✓	19.15 (13.60)	28.50 (22.30)	3.78 (2.00)	13.40 (8.30)
✓	✓	✓		16.71 (10.60)	23.71 (16.00)	2.80 (1.20)	12.03 (6.60)
✓	✓			13.66 (9.20)	23.99 (17.40)	2.31 (1.40)	10.57 (7.50)
✓		✓		3.78 (2.10)	10.91 (7.40)	0.37 (0.30)	7.55 (4.30)
	✓	✓		11.34 (6.30)	20.10 (12.90)	2.07 (1.10)	12.74 (7.30)

Table 2: **Ablation study for each component of MOCA.** For each metric, we report the corresponding path weighted scores in parentheses. The absence of checkmark denotes that a corresponding component is removed from MOCA.

Model	Validation-Seen		Validation-Unseen	
	Task	Goal-Cond	Task	Goal-Cond
MOCA (Ours)	19.15 (13.60)	28.50 (22.30)	3.78 (2.00)	13.40 (8.30)
- w/o I.A.T.	10.61 (7.10)	20.34 (15.60)	1.46 (0.80)	10.52 (6.60)
- w/o O.D.	16.10 (11.40)	23.80 (19.30)	3.53 (1.80)	12.41 (8.40)

Table 3: **Ablation for Instance Association in Time and Obstruction Detection.** Both Instance Association in Time and Obstruction Detection are ablated on the validation dataset.

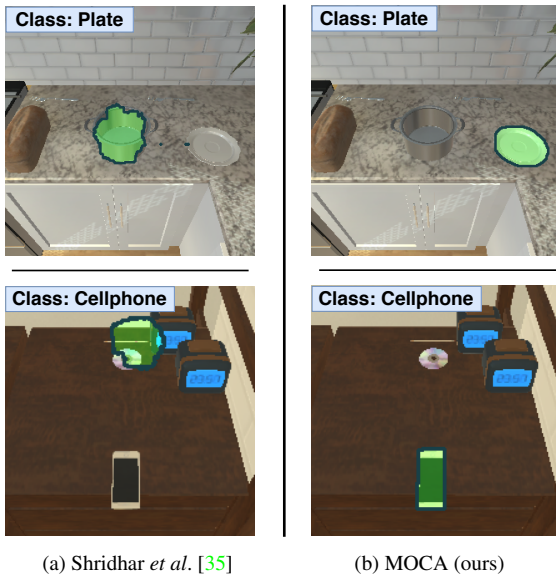


Figure 5: **Qualitative comparison of identifying target objects by mask prediction.** Green regions denote the interaction masks predicted by the model. The ground-truth object class the agent needs to interact with is shown on the top-left corner.

to the lack of cross-modal correspondence between visual and language inputs in the absence of dynamic filters.

Third, we demonstrate the importance of decoupling APM and VPM (Sec. 3.1). To remove the benefit of the decoupling, we take the concatenation of the goal-statement and instructions as the language input and perform action and mask prediction from the same pipeline similar to [35] while keeping other modules the same. The ablated model exhibits a drastic decrease in task success rates indicating

its inability to fully utilise the language inputs due to joint processing for mask and action module.

Finally, we remove object-centric mask prediction (Sec. 3.2). Instead, we directly upsample the joint vision-language-action embedding using deconvolution layers to predict the interaction mask similar to Shridhar *et al.* [35]. We observe that the performance drastically drops on both seen and unseen folds due to poor mask generation ability as indicated in Table 2, highlighting the effectiveness of our object-centric mask prediction module to consistently predict an accurate interaction mask.

Table 3 ablates the obstruction detection module from Sec. 3.4. The performance drop indicates that it is able to help the agent avoid obstacles effectively. We also ablate over the Instance-Association in Time (IAT) presented in Sec. 3.2.2. For this setting, instead of picking the mask instance for the predicted target class using IAT, we pick a random instance of that class. This setting achieves almost half the performance of MOCA which highlights that merely predicting the right object class is not sufficient, the correct instance should also be selected.

4.3. Qualitative Analysis

We conduct qualitative analysis on the interaction mask prediction ability (Sec. 3.2) of our agent MOCA. Our *Object-Centric Mask Prediction* allows MOCA to reason about object classes (Sec. 3.2.1) which ensures that it interacts with the right object. This is in contrast with [35] that upsamples a linear embedding via a deconvolution network and trains it to predict class-agnostic masks, thereby not preserving any information about object category. In Figure 5a, since [35] lacks the ability to reason about object class, it predicts inaccurately localized masks even though both the objects are fully observable.

In contrast, in Figure 5b, MOCA successfully predicts what objects it intends to interact with (*i.e.*, the cellphone and plate). Identifying the correct objects enables it to predict an accurately localised mask with the mask generator’s help. We present further ablation on the importance of reasoning about object classes and qualitative example videos of our agent’s task completion ability in the supplementary.

5. Conclusion

We explore the problem of interactive instruction following on the ALFRED benchmark. To address individual challenges in this compositional task, we propose, a modular object-centric approach, MOCA that exploits a modular design, an object-centric perspective on interaction, and flexible multimodal correspondence. MOCA outperforms all prior arts by large margins with superior generalization performance. Our framework presents a pathway for future work on this benchmark by giving the flexibility to work on upgrading individual components of the architecture.

References

- [1] Peter Anderson, Angel X. Chang, Devendra Singh Chaplot, Alexey Dosovitskiy, Saurabh Gupta, Vladlen Koltun, Jana Kosecka, Jitendra Malik, Roozbeh Mottaghi, Manolis Savva, and Amir R. Zamir. On evaluation of embodied navigation agents. *arXiv*, arXiv:1807.06757, 2018. 6
- [2] Peter Anderson, Qi Wu, Damien Teney, Jake Bruce, Mark Johnson, Niko Sünderhauf, Ian Reid, Stephen Gould, and Anton van den Hengel. Vision-and-language navigation: Interpreting visually-grounded navigation instructions in real environments. In *CVPR*, 2018. 1, 2
- [3] Angel Chang, Angela Dai, Thomas Funkhouser, Maciej Halber, Matthias Niessner, Manolis Savva, Shuran Song, Andy Zeng, and Yinda Zhang. Matterport3d: Learning from rgb-d data in indoor environments. *arXiv*, arXiv:1709.06158, 2017. 1
- [4] Devendra Singh Chaplot, Kanthashree Mysore Sathyendra, Rama Kumar Pasumarthi, Dheeraj Rajagopal, and Ruslan Salakhutdinov. Gated-attention architectures for task-oriented language grounding. In *AAAI*, 2017. 1, 2
- [5] Howard Chen, Alane Suhr, Dipendra Misra, Noah Snaveley, and Yoav Artzi. Touchdown: Natural language navigation and spatial reasoning in visual street environments. In *CVPR*, 2019. 1, 2
- [6] Kan Chen, Rama Kovvuri, and Ram Nevatia. Query-guided regression network with context policy for phrase grounding. In *ICCV*, 2017. 3
- [7] Marc-Alexandre Côté, Ákos Kádár, Xingdi Yuan, Ben Kybartas, Tavian Barnes, Emery Fine, James Moore, Matthew J. Hausknecht, Layla El Asri, Mahmoud Adada, Wendy Tay, and Adam Trischler. Textworld: A learning environment for text-based games. In *CGW@IJCAI*, 2018. 2
- [8] Abhishek Das, Samyak Datta, Georgia Gkioxari, Stefan Lee, Devi Parikh, and Dhruv Batra. Embodied Question Answering. In *CVPR*, 2018. 1
- [9] Kuan Fang, Alexander Toshev, Li Fei-Fei, and Silvio Savarese. Scene memory transformer for embodied agents in long-horizon tasks. In *CVPR*, 2019. 1
- [10] Daniel Fried, Ronghang Hu, Volkan Cirik, Anna Rohrbach, Jacob Andreas, Louis-Philippe Morency, Taylor Berg-Kirkpatrick, Kate Saenko, Dan Klein, and Trevor Darrell. Speaker-follower models for vision-and-language navigation. In *NeurIPS*, 2018. 2
- [11] Peng Gao, Pan Lu, Hongsheng Li, Shuang Li, Yikang Li, Steven Hoi, and Xiaogang Wang. Question-guided hybrid convolution for visual question answering. *arXiv*, arXiv:1808.02632, 2018. 2, 3, 5
- [12] Daniel Gordon, Aniruddha Kembhavi, Mohammad Rastegari, Joseph Redmon, Dieter Fox, and Ali Farhadi. Iqa: Visual question answering in interactive environments. In *CVPR*, 2018. 1
- [13] Kaiming He, Georgia Gkioxari, Piotr Dollár, and Ross Girshick. Mask r-cnn. In *ICCV*, 2017. 3, 6
- [14] Kaiming He, Xiangyu Zhang, Shaoqing Ren, and Jian Sun. Deep residual learning for image recognition. In *CVPR*, 2016. 6
- [15] Ronghang Hu, Marcus Rohrbach, Jacob Andreas, Trevor Darrell, and Kate Saenko. Modeling relationships in referential expressions with compositional modular networks. In *CVPR*, 2017. 3, 5
- [16] Ronghang Hu, Marcus Rohrbach, and Trevor Darrell. Segmentation from natural language expressions. In *ECCV*, 2016. 2
- [17] Ronghang Hu, Huazhe Xu, Marcus Rohrbach, Jiashi Feng, Kate Saenko, and Trevor Darrell. Natural language object retrieval. In *CVPR*, 2016. 2, 3, 4, 5
- [18] Xu Jia, Bert De Brabandere, Tinne Tuytelaars, and Luc Gool. Dynamic filter networks. In *NeurIPS*, 2016. 2, 5
- [19] Liyiming Ke, Xiujun Li, Yonatan Bisk, Ari Holtzman, Zhe Gan, Jingjing Liu, Jianfeng Gao, Yejin Choi, and Siddhartha Srinivasa. Tactical rewind: Self-correction via backtracking in vision-and-language navigation. In *CVPR*, 2019. 2
- [20] Eric Kolve, Roozbeh Mottaghi, Winson Han, Eli VanderBilt, Luca Weihs, Alvaro Herrasti, Daniel Gordon, Yuke Zhu, Abhinav Gupta, and Ali Farhadi. AI2-THOR: An Interactive 3D Environment for Visual AI. *arXiv*, arXiv:1712.05474, 2017. 1, 6
- [21] Jacob Krantz, Erik Wijmans, Arjun Majumdar, Dhruv Batra, and Stefan Lee. Beyond the nav-graph: Vision-and-language navigation in continuous environments. *arXiv*, arXiv:2004.02857, 2020. 1, 2
- [22] Federico Landi, Lorenzo Baraldi, Massimiliano Corsini, and Rita Cucchiara. Embodied vision-and-language navigation with dynamic convolutional filters. In *BMVC*, 2019. 2
- [23] Xiujun Li, Chunyuan Li, Qiaolin Xia, Yonatan Bisk, Asli Çelikyilmaz, Jianfeng Gao, Noah A. Smith, and Yejin Choi. Robust navigation with language pretraining and stochastic sampling. In *EMNLP/IJCNLP*, 2019. 2
- [24] Jingyu Liu, Liang Wang, and Ming-Hsuan Yang. Referring expression generation and comprehension via attributes. In *ICCV*, 2017. 3
- [25] Chih-Yao Ma, Jiasen Lu, Zuxuan Wu, Ghassan AlRegib, Zolt Kira, Richard Socher, and Caiming Xiong. Self-monitoring navigation agent via auxiliary progress estimation. In *ICLR*, 2019. 2
- [26] Chih-Yao Ma, Zuxuan Wu, Ghassan AlRegib, Caiming Xiong, and Zolt Kira. The regretful agent: Heuristic-aided navigation through progress estimation. In *CVPR*, 2019. 2
- [27] Matt MacMahon, Brian Stankiewicz, and Benjamin Kuipers. Walk the talk: Connecting language, knowledge, and action in route instructions. In *AAAI*, 2006. 2

- [28] Manolis Savva*, Abhishek Kadian*, Oleksandr Maksymets*, Yili Zhao, Erik Wijmans, Bhavana Jain, Julian Straub, Jia Liu, Vladlen Koltun, Jitendra Malik, Devi Parikh, and Dhruv Batra. Habitat: A Platform for Embodied AI Research. In *ICCV*, 2019. [1](#)
- [29] Dipendra Misra, John Langford, and Yoav Artzi. Mapping instructions and visual observations to actions with reinforcement learning. In *EMNLP*, 2017. [1](#)
- [30] Varun K Nagaraja, Vlad I Morariu, and Larry S Davis. Modeling context between objects for referring expression understanding. In *ECCV*, 2016. [3](#)
- [31] Hyeonwoo Noh, Paul Hongsuck Seo, and Bohyung Han. Image question answering using convolutional neural network with dynamic parameter prediction. In *CVPR*, 2016. [3](#)
- [32] Cristian Rodriguez-Opazo, Edison Marrese-Taylor, Fatemeh Saleh, Hongdong Li, and Stephen Gould. Proposal-free temporal moment localization of a natural-language query in video using guided attention. In *WACV*, 2020. [5](#)
- [33] Anna Rohrbach, Marcus Rohrbach, Ronghang Hu, Trevor Darrell, and Bernt Schiele. Grounding of textual phrases in images by reconstruction. In *ECCV*, 2016. [2, 3](#)
- [34] Evan Shelhamer, Jonathan Long, and Trevor Darrell. Fully convolutional networks for semantic segmentation. In *IEEE TPAMI*, 2017. [3](#)
- [35] Mohit Shridhar, Jesse Thomason, Daniel Gordon, Yonatan Bisk, Winson Han, Roozbeh Mottaghi, Luke Zettlemoyer, and Dieter Fox. Alfred: A benchmark for interpreting grounded instructions for everyday tasks. In *CVPR*, 2020. [1, 2, 3, 4, 5, 6, 7, 8, 11, 12](#)
- [36] Mohit Shridhar, Xingdi Yuan, Marc-Alexandre Côté, Yonatan Bisk, Adam Trischler, and Matthew Hausknecht. ALFWorld: Aligning Text and Embodied Environments for Interactive Learning. *arXiv*, arXiv:2010.03768, 2020. [2](#)
- [37] Hao Tan, Licheng Yu, and Mohit Bansal. Learning to navigate unseen environments: Back translation with environmental dropout. In *NAACL*, 2019. [2](#)
- [38] Takayuki Okatani Van-Quang Nguyen. A hierarchical attention model for action learning from realistic environments and directives. *ECCV EVAL Workshop*, <https://askforalfred.com/EVAL/>, 2020. [2, 7](#)
- [39] Harm D. Vries, Florian Strub, Jérémie Mary, Hugo Larochelle, Olivier Pietquin, and Aaron C. Courville. Modulating early visual processing by language. *arXiv*, arXiv:1707.00683, 2017. [3](#)
- [40] Liwei Wang, Yin Li, and Svetlana Lazebnik. Learning deep structure-preserving image-text embeddings. In *CVPR*, 2016. [3](#)
- [41] Xin Wang, Wenhan Xiong, Hongmin Wang, and William Yang Wang. Look before you leap: Bridging model-free and model-based reinforcement learning for planned-ahead vision-and-language navigation. In *ECCV*, 2018. [2](#)
- [42] Fanbo Xiang, Yuzhe Qin, Kaichun Mo, Yikuan Xia, Hao Zhu, Fangchen Liu, Minghua Liu, Hanxiao Jiang, Yifu Yuan, He Wang, Li Yi, Angel X. Chang, Leonidas J. Guibas, and Hao Su. Sapien: A simulated part-based interactive environment. In *CVPR*, 2020. [1](#)
- [43] Licheng Yu, Zhe Lin, Xiaohui Shen, Jimei Yang, Xin Lu, Mohit Bansal, and Tamara L. Berg. Mattnet: Modular attention network for referring expression comprehension. In *CVPR*, 2018. [2, 3, 4](#)
- [44] Licheng Yu, Patrick Poirson, Shan Yang, Alexander C. Berg, and Tamara L. Berg. Modeling context in referring expressions. In *ECCV*, 2016. [3](#)
- [45] Yuke Zhu, Daniel Gordon, Eric Kolve, Dieter Fox, Li Fei-Fei, Abhinav Gupta, Roozbeh Mottaghi, and Ali Farhadi. Visual semantic planning using deep successor representations. In *ICCV*, 2017. [1](#)
- [46] Charles Lawrence Zitnick and Piotr Dollár. Edge boxes: Locating object proposals from edges. In *ECCV*, 2014. [3](#)

Appendix

A. Quantitative Analysis on Task-Type and Sub-goal performance

The tasks in ALFRED [35] are divided into 7 high-level categories. Table 4 shows the performance of MOCA on each task type. On short-horizon tasks such as **Pick & Place** and **Examine**, Shridhar *et al.* achieve some success in seen environments, but have near zero unseen success rates. However, MOCA outperforms them on both these task types in both seen and unseen scenes by large margins. **Stack & Place** and **Pick Two & Place** are the two most complex and the longest horizons task types in ALFRED. MOCA achieves 5.2% and 11.2% seen success rate as compared to 0.9% and 0.8% of Shridhar *et al.* [35]. It also achieves some success in unseen scenes whereas Shridhar *et al.* show zero unseen success rates.

Following [35], we also examine the performance of MOCA on individual sub-goals. For sub-goal analysis, we use the expert trajectory to move the agent to the starting time step of the respective sub-goal. Then the agent starts inference based on the current observations. Table 5 shows the agent’s performance on individual sub-goals. **Goto** subgoal is indicative of the navigation ability of an agent. Even though navigation in unseen, visually complex environments is more challenging, our model achieves 32% as opposed to 22% of Shridhar *et al.* [35]. Although the gap between average sub-goal performance of Shridhar *et al.* and MOCA is relatively small, MOCA drastically outperforms it on full task completion as shown in Table 1 of the main paper. This indicates MOCA’s ability to succeed on overall task completion and not limiting itself to memorizing short term sub-goals only.

B. Analysis on Object Class Reasoning

We investigate the importance of reasoning about object categories by removing the target class prediction stage from our *Object-Centric Mask Prediction*. For this ablation, our agent selects the mask instance with the highest confidence score across all classes (*i.e.* without class prediction of a target object). We observe that this leads to a huge drop in performance as the agent tries to interact with incorrect objects and hence fails to accomplish most of the tasks. Specifically, success rate in *Seen* drops from 19.15% to 0.37% and in *Unseen* drops from 3.78% to 0.24%. This is indicative of the importance of explicitly enabling our agent to condition its mask prediction on object class information.

C. Qualitative Analysis of Task Completion

We present qualitative examples of the task completion ability of our agent and contrast it with Shridhar *et al.* [35] in the attached videos. Each frame the videos includes the

Task-Type	Shridhar <i>et al.</i> [35]		MOCA (ours)	
	Seen	Unseen	Seen	Unseen
Pick & Place	7.0	0.0	29.5	5.0
Cool & Place	4.0	0.0	26.1	0.7
Stack & Place	0.9	0.0	5.2	1.8
Heat & Place	1.9	0.0	15.8	2.7
Clean & Place	1.8	0.0	22.3	2.4
Examine	9.6	0.0	20.2	13.2
Pick Two & Place	0.8	0.0	11.2	1.1
Average	3.7	0.0	18.6	3.8

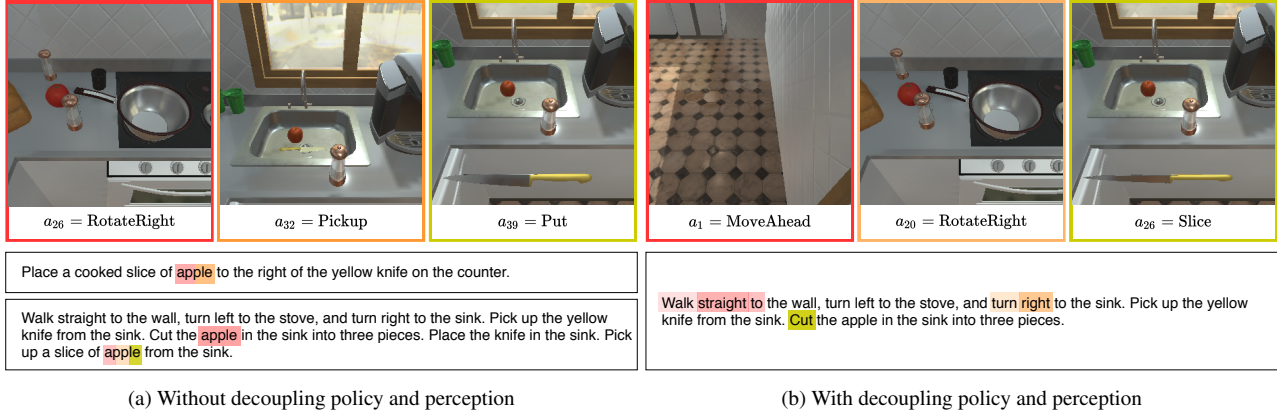
Table 4: **Success Rates across 7 task types in ALFRED.** All values are in percentage. The agent is evaluated on the Validation set. Highest values per fold are indicated in **blue**.

Sub-Goal	Shridhar <i>et al.</i> [35]		MOCA (ours)	
	Seen	Unseen	Seen	Unseen
Goto	51	22	54	32
Pickup	32	21	53	44
Put	81	46	62	39
Cool	88	92	87	38
Heat	85	89	84	86
Clean	81	57	79	71
Slice	25	12	51	55
Toggle	100	32	93	11
Average	68	46	70	47

Table 5: **Sub-goal success rate.** The highest values per fold and task are shown in **blue**.

goal statement and step-by-step instructions. The step-by-step instruction that the agent tries to accomplish at the current time step is highlighted in yellow. When our agent MOCA performs interaction, the predicted target class of the object at that time step is shown on the top-left corner of the egocentric frame. Note we do not show object class for Shridhar *et al.* [35] since they produce class-agnostic masks. We present both success and failure cases of our agent. In *success_1.mp4*, while Shridhar *et al.* [35] fails to navigate to right object *i.e.* yellow spray bottles, MOCA successfully navigates and places both of them on top of the toilet, thereby satisfying the goal statement. It indicates our Action Policy Module’s (APM) ability to predict an accurate action sequence based on vision and language inputs.

For *success_2.mp4*, both MOCA and Shridhar *et al.* [35] navigate correctly to the right locations at various stages of the task. However when the instruction asks to pick up the lettuce, MOCA correctly localizes and picks up the correct object. The visual perception module (VPM) of MOCA which enables it to reason about object classes helps it to predict the mask of the correct object *i.e.* lettuce. On the contrary, Shridhar *et al.* [35] picks up a cup which was not



(a) Without decoupling policy and perception

(b) With decoupling policy and perception

Figure 6: **Language attention at various frames with and without decoupling policy and perception.** The colors of frame borders and words denote that the agent at the particular frame focuses on the same-colored words. a_t denotes the action taken at time step t . (a) Without decoupling, the language attention of the agent keeps focusing on *apple* irrespective of the action taken. (b) With decoupling, the language attention focuses on the words that correspond to the action taken at that time step.

mentioned in the instruction at all, thereby failing on the tasks even though it performs all the other actions accurately. This can be attributed to its class-agnostic nature of interaction mask prediction. Similarly in *success_3.mp4*, while Shridhar *et al.* [35] fails to pick up the knife, due to an inaccurately localized mask under limited visibility and picks up the spatula instead, MOCA rightly picks up the knife and successfully accomplishes the task. *success_4.mp4* also shows a similar example.

success_5.mp4 demonstrates the ability to perform the tasks in a more efficient manner. Even though Shridhar *et al.* [35] successfully navigates to the cup, it takes a lot of unnecessary navigation actions which harms the path-length-weighted score. After picking up the cup it fails to navigate further and ends up being stuck at a desk and therefore fails. If our agent, MOCA would've faced a similar scenario, our Obstruction Detection module would have kicked in and helped the agent to evade it. On the other hand, MOCA navigates to the correct objects of interest *i.e.*, the cup, the refrigerator, and a counter. It also performs accurate interactions and therefore accomplishes the given task.

For the *fail.mp4* video, Shridhar *et al.* [35] tries to interact with an irrelevant object (cloth), instead of the tissue box and fails at completing the task. Similarly, our agent, MOCA also tries to interact with the wrong target object (soap bottle), as it fails to navigate to the right position to observe that object, making it invisible to it. This misleads the VPM to perceive the soap bottle as a tissue box and therefore tries to place an unintended object on top of a toilet and failing the task.

D. Benefit of Decoupling Policy and Perception

We observe that when the same pipeline for action and mask prediction is used in a similar way as Shridhar *et*

al. [35], the language attention tends to focus on words that are common between the goal and step-by-step instructions, missing on important low-level action information. The decoupling of policy and perception in MOCA allows the agent to focus on relevant words and hence effectively utilise the instructions for accurate action prediction. Figure 6 qualitatively illustrates this observation. In Figure 6a, for the case without decoupling, the attention keeps focusing on the objects mentioned in the goal statement, such as the apple, even when it is not relevant to the current action ignoring all other low-level action-specific information. Contrastingly, when both the pipelines are decoupled, the attention mechanism focuses on the correct words. For example, at $t = 20$ it attends over *turn right* when our agent, MOCA predicts ROTATERIGHT. At $t = 26$ when our agent intends to slice the apple slice, it attends over *Cut*.